13. Lunar Portable Magnetometer Experiment

P. Dyal,[a]† *C. W. Parkin,*[a b] *C. P. Sonett,*[a] *R. L. DuBois,*[c] *and G. Simmons*[d]

The Apollo 14 lunar portable magnetometer (LPM) (fig. 13–1) was used to measure the steady magnetic field at different sites in the Fra Mauro region. The LPM recorded steady magnetic fields of 103 ± 5 gammas and 43 ± 6 gammas at two sites separated by 1.12 km. These measurements showed that the unexpectedly high 38-gamma steady field measured [1] at the Apollo 12 site 180 km away (ref. 13–1) was not unique. Indeed, these measurements and studies of lunar samples [2,3] (refs. 13–2 to 13–5) and lunar-orbiting Explorer 35 data (ref. 13–6) indicate that much of the lunar-surface material was magnetized at some prior time in lunar history. These data can be used to gain information concerning present magnetic and structural properties of the local region as well as the thermal and magnetic histories of the area.

Background and Theory of the Experiment

Magnetic fields are believed to permeate most of space, and forces associated with these fields are very important on a cosmological scale. In this solar system, strong magnetic fields associated with sunspot regions extend far enough to affect radio reception and auroral activity on the Earth. The dipolar field of the Earth acts as a shield against the hot solar plasma by deflecting it around the terrestrial sphere. Magnetic-field measurements on the surface of the Earth have a wide range of application (e.g., in navigation; paleomagnetic studies of the geological past, such as sea-floor spreading; and surveys of subsurface ore bodies).

The magnitudes of magnetic fields in the universe vary widely. Measurements range from ap-

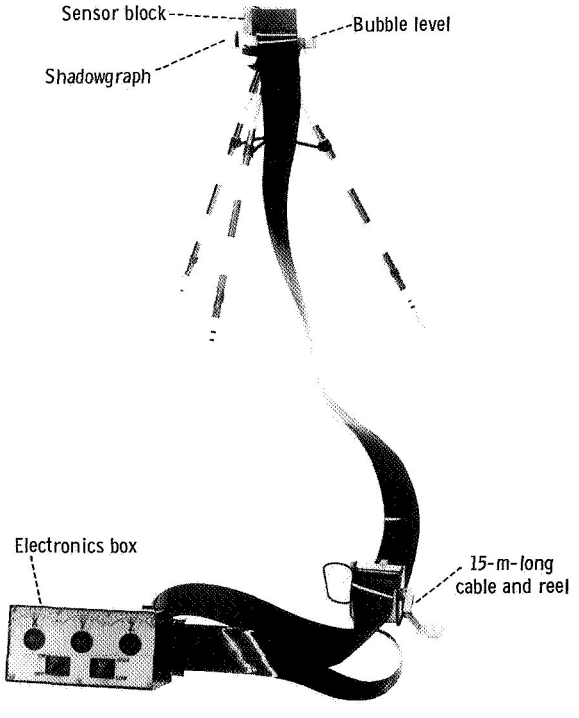

FIGURE 13–1.—The LPM deployed in the laboratory.

[a] NASA Ames Research Center.
[b] National Research Council postdoctoral associate.
[c] Oklahoma University.
[d] NASA Manned Spacecraft Center and Massachusetts Institute of Technology.
† Principal investigator.

[1] P. Dyal and C. W. Parkin: The Apollo 12 Magnetometer Experiment: Internal Lunar Properties From Transient and Steady Magnetic Field Measurements. Proc. Apollo 12 Lunar Sci. Conf. (Houston), Jan. 11–14, 1971. To be published in Geochim. Cosmochim. Acta.

[2] G. W. Pearce, D. W. Strangway, and E. E. Larson: Magnetism of Two Apollo 12 Igneous Rocks. Proc. Apollo 12 Lunar Sci. Conf. (Houston), Jan. 11–14, 1971. To be published in Geochim. Cosmochim. Acta.

[3] C. E. Helsley: Evidence for an Ancient Lunar Magnetic Field. Proc. Apollo 12 Lunar Sci. Conf. (Houston), Jan. 11–14, 1971. To be published in Geochim. Cosmochim. Acta.

proximately 10^{12} gammas for a white dwarf star in the constellation Draconis (ref. 13–7) to approximately 10^{8} gammas inside sunspots (ref. 13–8) to 5 gammas in interplanetary space near the Earth (ref. 13–9). The Earth surface field near the Equator is approximately 30 000 gammas, and the fields measured at three lunar-surface sites average about 60 gammas. The sources of these fields are associated with the intrinsic physical properties of materials or moving electrical charges.

Magnetic fields associated with the Moon have been found to be much more important to lunar studies than had been anticipated before the Apollo lunar-landing missions. The inductive response of the lunar interior to time-dependent solar-magnetic fields transported past the Moon permits the present electromagnetic and thermal properties of the lunar interior to be studied (refs. 13–10 and 13–11). Present and future Apollo missions will yield information about the past extrinsic and intrinsic magnetic fields and help clarify major events in lunar history. Past extrinsic fields will have been influential during lunar formation, and the study of the resultant remanence should yield information about ancient solar and terrestrial fields. Intrinsic fields should yield information concerning the history of lunar internal temperature, rotation, volcanism, and tectonic processes.

During the last decade, many investigators (refs. 13–12 to 13–16) conducted experiments to determine the magnetic field associated with the Moon. These experiments, conducted aboard lunar-orbiting and flyby spacecraft, yielded no direct measurement of an intrinsic magnetic field. One of the lunar-orbiting experiments, Explorer 35, aided directly in the LPM experiment. During the second period of astronaut extravehicular activity (EVA), the Explorer 35 recorded the time-independent ambient magnetic field caused by external sources (fig. 13–2). The Explorer 35 measurements, made simultaneously with the LPM measurements, were later vectorially subtracted from the LPM data.

Before the Apollo 14 mission, the measurements made by the Explorer 35 and other lunar-orbiting and flyby spacecraft were an aid in establishing a maximum limit of 4 gammas for an assumed intrinsic global magnetic field. It was, therefore,

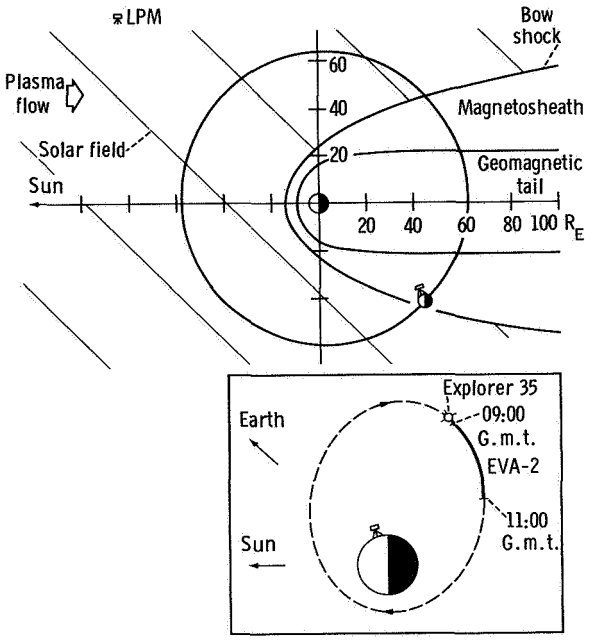

FIGURE 13–2.—The lunar orbit projected onto the ecliptic plane, showing the position of the Apollo 14 LPM on February 6, 1971, during the time of LPM magnetic-field measurements. The inset shows the orbit and location of the Explorer 35 satellite at the time of the surface measurements.

surprising to measure a 38-gamma steady field at the Apollo 12 landing site. This was the first direct surface measurement of a magnetic field intrinsic to an extraterrestrial planetary-sized body.

The magnetic field is probably due to magnetized material that acquired remanence during a lunar epoch involving an inducing field much larger ($\geqq 10^{3}$ gammas) than presently exists at the Moon. This conclusion is consistent with the high remanent magnetization found in lunar samples.

Discovery of the unexpectedly high steady field at the Apollo 12 site resulted in the concept of the Apollo 14 LPM experiment. This instrument was designed to make multiple measurements of the steady (time-independent) magnetic field during the astronauts' traverse at their landing site. The entire project from inception to data return required slightly more than 1 yr. The effort was rewarded by the measurement at Fra Mauro of a 103-gamma field—approximately 25 times greater than had been predicted only 15 months before.

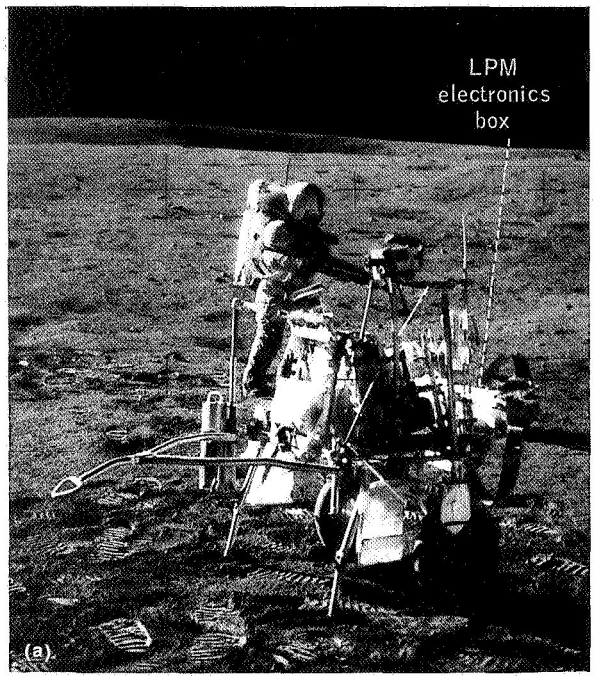

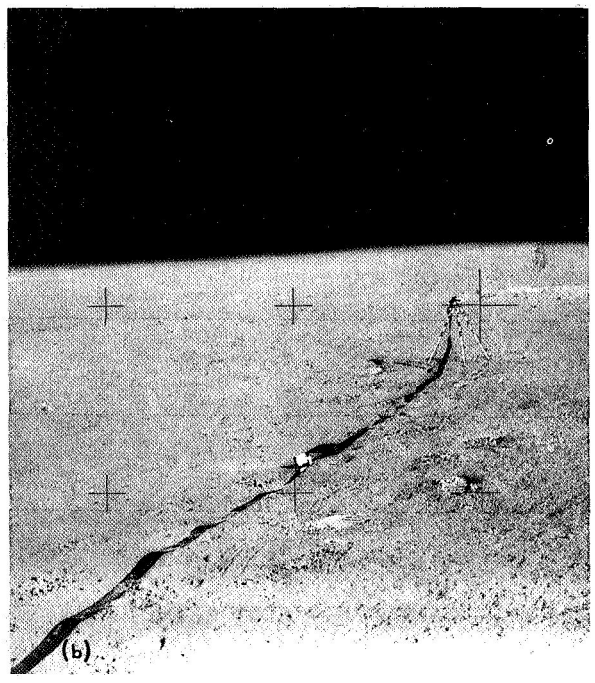

FIGURE 13–3.—Apollo 14 LPM on the lunar surface. (a) On the MET. (b) Deployed at site A during measurement of the 103-gamma magnetic field.

Equipment Description

The LPM was designed as a totally self-contained, portable experiment package. During transit from the Earth to the Moon, the LPM was stowed and attached to the scientific equipment bay of the lunar module (LM); and, on the lunar surface, the LPM was carried on the modularized equipment transporter (MET) (fig. 13–3(a)). In the deployed configuration (fig. 13–3(b)), three orthogonal fluxgate sensors are mounted on top of a tripod. This sensor-equipped tripod is connected by a 15-m-long ribbon cable to the electronics box that contains a battery pack, electronics package, and three milliammeters. (A list of pertinent LPM characteristics is given in table 13–I.)

Fluxgate Sensor

The fluxgate sensor, shown schematically in figure 13–4, records the vector components of the magnetic field. Three fluxgate sensors (refs. 13–17 and 13–18) are orthogonally mounted in the sensor block shown in figure 13–1. Each sensor weighs 18 g and uses 15 mW of power during operation. A sensor consists of a flattened toroidal core of Permalloy that is driven to saturation by a square wave at a frequency of $f_0 = 7250$ Hz. This constant-voltage square wave drives the core to saturation during alternate half-cycles and modulates the permeability at twice the drive frequency. The voltage induced in the sense windings

TABLE 13–I. *Apollo 14 LPM Characteristics*

Parameter	*Value*
Ranges, gamma	0 to ±100 0 to ±50
Resolutions, gamma	±1.0, ±0.5
Frequency response, Hz	dc to 0.01
Battery:	
Power, W	1.5
Life, hr	60
Mass, kg	4.58
Stowage size, cm	55.9×15.3×14.3
Operating temperature, °C	−30 to +60°
Angular response	Proportional to cosine of angle between sensor axis and magnetic field

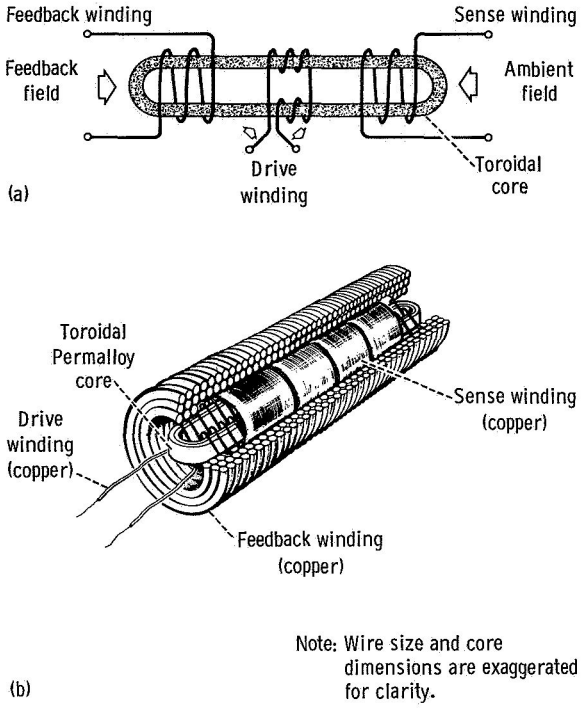

FIGURE 13–4.—Fluxgate sensor. (a) Functional schematic. (b) Racetrack tape 0.0005 in. thick and 0.0625 in. wide.

is equal to the time rate of change of the net flux contained in the area enclosed by the sense winding. This net flux is the superposition of the flux from the drive winding and the ambient magnetic field. The signal generated in the sense winding at the second harmonic of the drive signal will be amplitude modulated at a magnitude proportional to the ambient magnetic field. The phase of this second harmonic signal, with respect to the drive waveform, indicates the polarity of the magnetic field. The sensor electronics amplify and filter the $2f_0$ sense-winding signal and synchronously demodulate it to derive a voltage proportional to the ambient magnetic field. After demodulation, the resulting signal is amplified and used to drive the feedback winding to null out the ambient field within the sensor. Operating at null increases thermal stability by making the circuit independent of core-permeability variations with temperature.

The sensor block, mounted on the top of a tripod, is positioned 75 cm above the lunar surface. The tripod assembly consists of a latching device to hold the sensor block, a bubble level with 1° annular rings, and a shadowgraph with 3° markings used to aline the device along the Moon-Sun line.

Electronics Subsystem

The magnetometer electronics are self-contained with a set of mercury cells for power and three milliammeters for visual readout of the magnetic-field components. A block diagram of the instrument is shown in figure 13–5. The sensors are driven into saturation by a 7.25-kHz square wave generated by a frequency-divided Colpitts oscillator operating at 29 kHz. The oscillator also provides a 14.5-kHz pulse for demodulation of the second harmonic signal from the sense windings. The amplifier-demodulator is a narrowband amplifier with 80-dB gain at 14.5 kHz. The amplifier output is synchronously demodulated, producing a direct-current (dc) output voltage proportional to the amplitude of the ambient magnetic field. This demodulated output is used to drive the feedback winding of the sensor to operate the sensor at null conditions. The demodulated output from each channel also drives a panel meter. Each

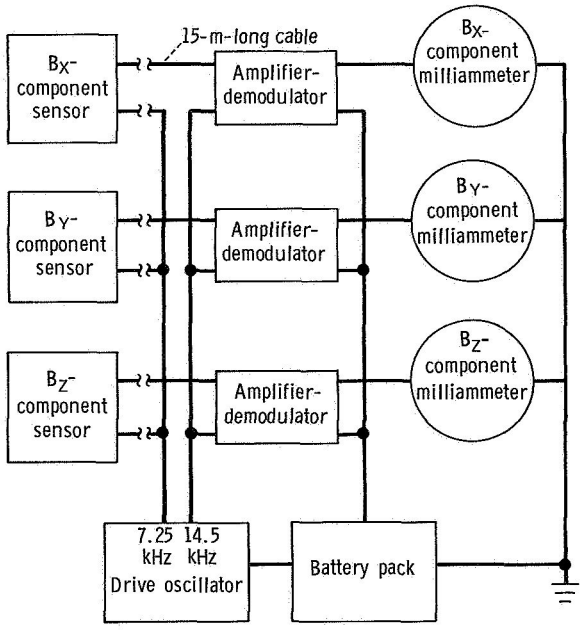

FIGURE 13–5.—Functional block diagram of the LPM electronics.

meter has a 1-mA full-scale movement and associated scaling resistors and capacitors that determine the frequency response of the instrument. This frequency response is chosen so that the instrument can follow changes in steady-field values between measurements at different sites but still filter out high-frequency fluctuations in the ambient solar-wind field. The instrument has an overall low-pass filter frequency response with a 3-dB point at 0.05 Hz. The meters also have a range switch connected to the scaling resistors to permit full-scale deflection for either ± 50 gammas or ± 100 gammas with reading-resolution capabilities of ± 1 and ± 2 gammas, respectively.

Exterior surfaces of the instrument were designed so that the temperatures of all components would be maintained between 0° and 50° C for Sun-elevation angles between 7° and 30°. The desired effective optical absorptance and emittance of the instrument were achieved by coating the surface areas with appropriate ratios of electrodeposited gold and white thermal paint. The temperature of the electronics box is measured by visually observing the darkening of temperature-sensitive decals that monitor temperatures in increments between 100° and 290° F.

Instrument Operation

Crew operations are crucial to the execution of this experiment. Both crewmembers remove the LPM mounting pallet from the LM and install the magnetometer on the MET. The MET is then transported a minimum of 100 m from the LM to eliminate the LM as an artificial field source. A measurement sequence is conducted as follows. Leaving the electronics box on the MET, the astronaut deploys the sensor-tripod assembly and levels and alines the sensor block a minimum of 11 m from the MET. He returns to the MET, sets the range switch at either 50 or 100 gammas, then reads the meters in sequence and verbally relays the data to Earth. After all readings are taken, the astronaut reels up the cable and stows the sensor-tripod assembly.

At the first site only, two sets of additional readings are taken with the sensor block rotated first 180° about a horizontal axis, then 180° about a vertical axis. These additional readings allow determination of a zero offset for each axis. Sensor offsets of vector magnetometers are inherently sensitive to environmental change; thus, a surface measurement of offsets is required. Gain and linearity, however, are relatively insensitive to environmental change.

Results

Magnetic-field measurements were conducted at two sites by the LM pilot during the second period of EVA on February 6. The first measurement was made approximately 170 m from the LM at site A (fig. 13–6), and the second was

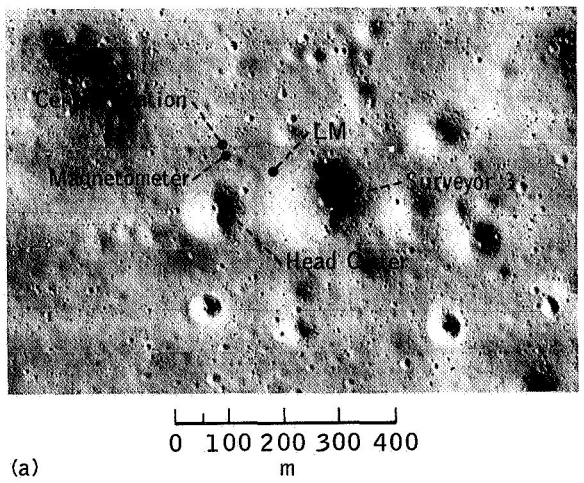

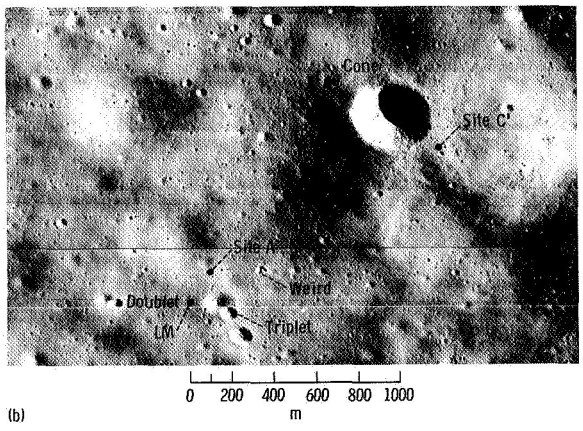

FIGURE 13–6.—Lunar Orbiter photographs showing the Apollo 12 and 14 landing sites and positions where steady-field measurements were made. (a) Apollo 12 site. (b) Apollo 14 site.

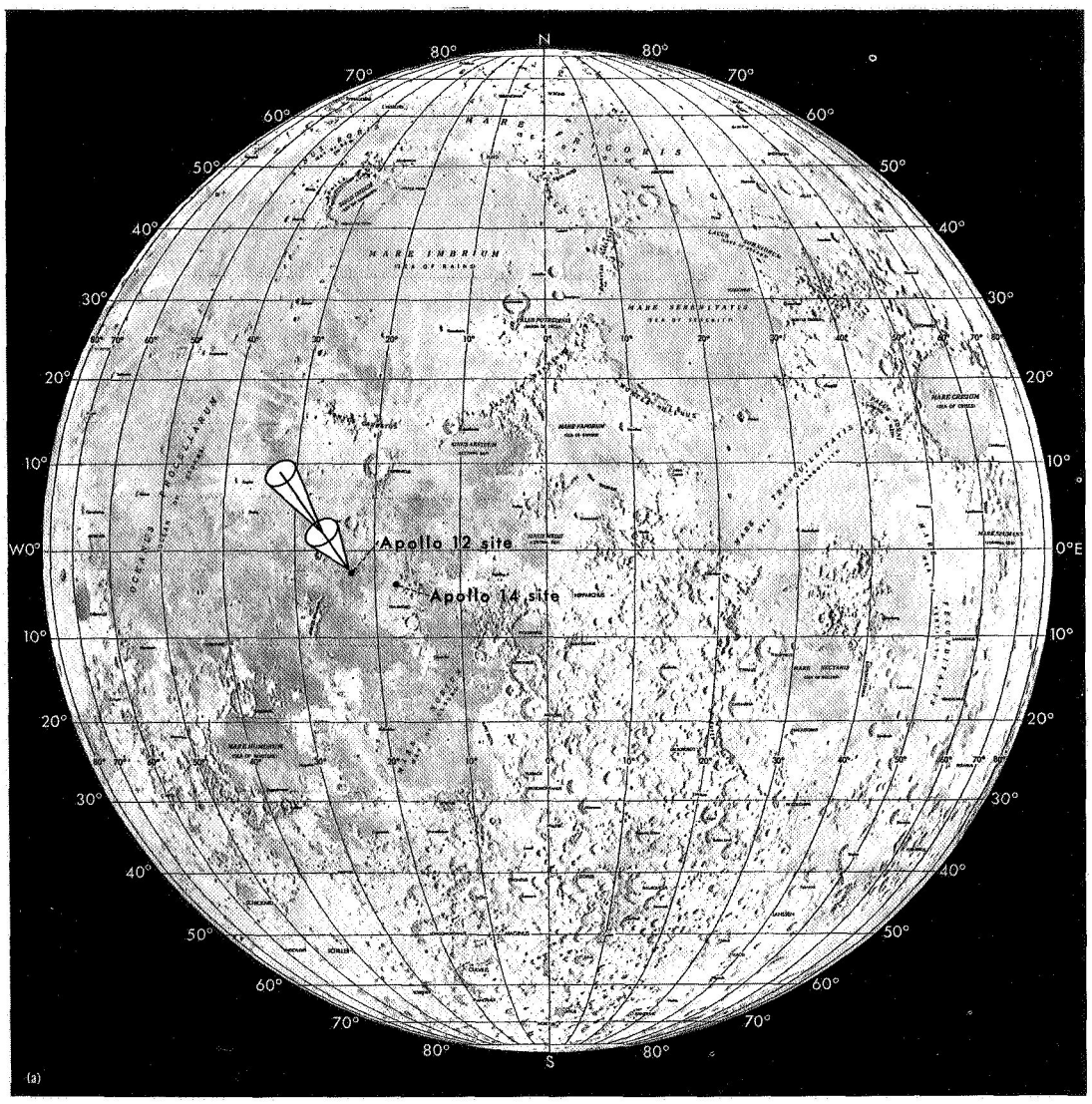

FIGURE 13–7.—Orientation of lunar magnetic-field measurements. (a) Relative location of the Apollo 14 and 12 landing sites.

made near the rim of Cone Crater at site C′. The vector magnetic-field components measured at each site are as follows. At site A, the total LPM-measured components are $B_X = -90$ gammas, $B_Y = 45$ gammas, and $B_Z = -30$ gammas. At site C′, components are $B_X = -11$ gammas, $B_Y = -28$ gammas, and $B_Z = -28$ gammas. These components are listed in a local coordinate system with the origin on the surface; the B_X-component is positive toward the zenith, and the B_Y- and B_Z-components are positive along the surface to the east and north, respectively.

The two Apollo 14 field measurements are each the vector sum of intrinsic lunar fields and the extralunar (solar or terrestrial or both) fields. The Explorer 35 magnetometer orbiting the Moon, as shown in figure 13–2, simultaneously makes measurements of the extralunar fields. To determine the intrinsic steady field at the two surface sites, it is necessary to transform these extralunar

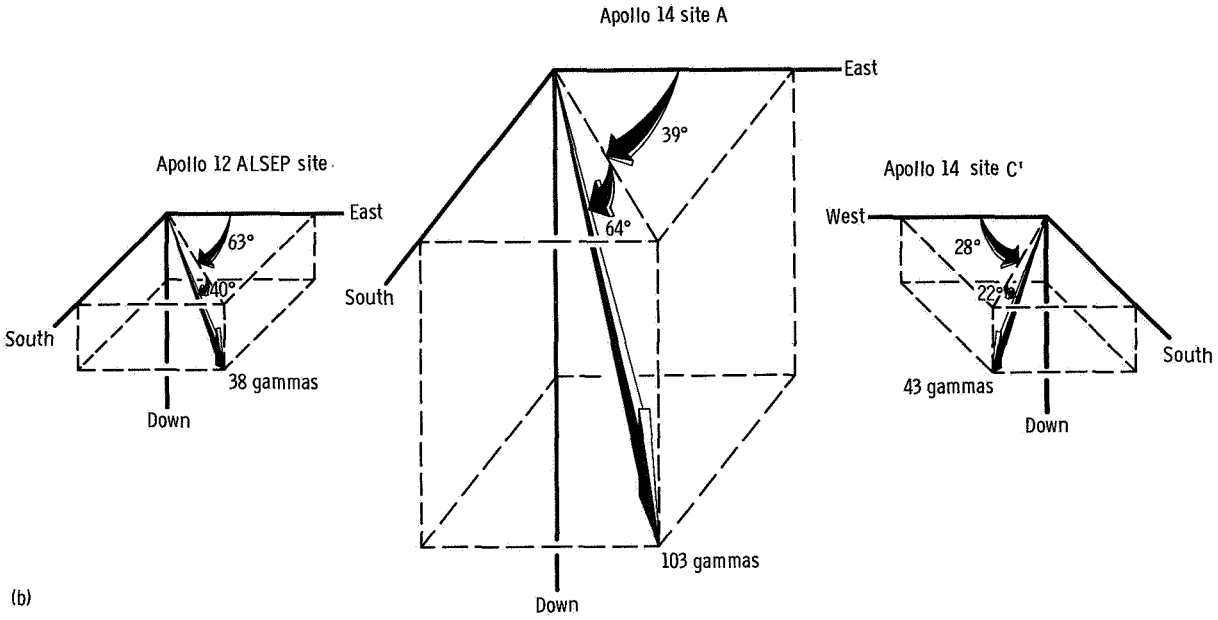

FIGURE 13–7.—Continued—(b) The vector fields for each of the three point measurements.

fields to the Apollo 14 surface coordinate system and vectorially subtract them from the LPM measurements.

In addition to the external fields measured by Explorer 35, there is a time-dependent inductive field generated in the Moon that is proportional to the amplitude and frequency of the Explorer 35 extralunar field (ref. 13–11) and that is not completely filtered out by the LPM. This inductive field must also be subtracted from the Apollo 14 measurements; it is determined by examination of past simultaneous Apollo 12 and Explorer 35 data measured in the same lunar-orbital position (fig. 13–2). The Apollo 12 lunar-surface magnetometer, which would have directly monitored these time-dependent inductive fields, was not operating at the time of the Apollo 14 mission.

The intrinsic lunar steady fields at the Apollo 14 site, which can be calculated by vectorial subtraction of extralunar and induction fields, are listed in table 13–II and are illustrated in figure 13–7. Errors listed in table 13–II include uncertainties in sensor orientation, instrument-temperature measurements, and inductive-field determination.

A magnetic-field gradient can be calculated

TABLE 13–II. *Magnetic-Field Measurements at Apollo 14 and 12 Sites*

Site	*Coordinates, deg*	*Field magnitude, gammas*	*Magnetic-field components, gammas*		
			Up	*East*	*North*
Apollo 14:	3.7° S, 17.5° W				
Site A.....	(See fig. 3.1 in sec. 3)	103±5	−93±4	+38±5	−24±5
Site C'.....	(See fig. 3.1 in sec. 3)	43±6	−15±4	−36±5	−19±8
Apollo 12 site.....	3.2° S, 23.4° W	38±3	−24.4±2.0	+13.0±1.8	−25.6±0.8

from the two Apollo 14 site measurements. Sites A and C′ are separated by 1.12 km (fig. 13–6(b)), and the linear gradient is calculated to be 54 ± 7 gammas/km. This value is less than the gradient upper limit determined for the Apollo 12 site 180 km away. At the Apollo 12 site, the steady field is measured to be 38 ± 3 gammas and the gradient upper limit is 133 gammas/km (ref. 13–1). These values are shown for reference in figure 13–7 and table 13–II.

Discussion

The two magnetic-field measurements at the Apollo 14 site have shown that the unexpectedly high field measured at the Apollo 12 site is not a feature confined to one site on the Moon. These three magnetometer measurement sites, separated by distances of from 1 to 180 km, and the high remanence found in the samples[4,5] returned from the Apollo 11 and 12 sites (refs. 13–2 to 13–5), separated by 1400 km, experimentally show that the Moon has been magnetized in these widely separated regions. It is quite possible that thousands of local surface regions of magnetized concentrations (magcons) may exist (ref. 13–19), and reexamination of the Explorer 35 magnetometer and plasma data indicates that several magnetized nonmare areas exist on both the near and far sides of the Moon (ref. 13–6). These analyses give evidence that much of the lunar-surface material has been magnetized—perhaps even a crustal shell around the entire Moon.

No obvious mechanism for such large-scale magnetization of surface materials exists at present. Magnetization of the Apollo 11 and 12 samples would have required an external field greater than 10^3 gammas (ref. 13–5). Ambient fields of this magnitude have not been measured in space near the Moon; the largest measured so far are transient fields of a magnitude of approximately 10^2 gammas; these transient fields last only a few minutes (ref. 13–20).

Sources of the Steady Field

The similarities between the Apollo 12 and 14 field measurements (viz, all vectors are pointed down and toward the south and have magnitudes that correspond to within a factor of 3) suggest that the two Apollo 14 sites and possibly the Apollo 12 site are located above a near-surface slab of material that was uniformly magnetized at one time. Subsequently, the magnetization in the slab was altered by local processes, such as tectonic activity or fracturing and shock demagnetization from meteorite impacts. This latter process is graphically illustrated in figure 13–8.

The Apollo 12 and 14 steady magnetic fields could also originate in surface or subsurface dipolar sources, such as meteoroid fragments or ore bodies. Properties of such a source assumed for the Apollo 12 field have been discussed in a previous work (ref. 13–1); a similar analysis will be performed for the Apollo 14 fields.

Numerous other source models exist that could

[4] G. W. Pearce, D. W. Strangway, and E. E. Larson: Magnetism of Two Apollo 12 Igneous Rocks. Proc. Apollo 12 Lunar Sci. Conf. (Houston), Jan. 11–14, 1971. To be published in Geochim. Cosmochim. Acta.

[5] C. E. Helsley: Evidence for an Ancient Lunar Magnetic Field. Proc. Apollo 12 Lunar Sci. Conf. (Houston), Jan. 11–14, 1971. To be published in Geochim Cosmochim. Acta.

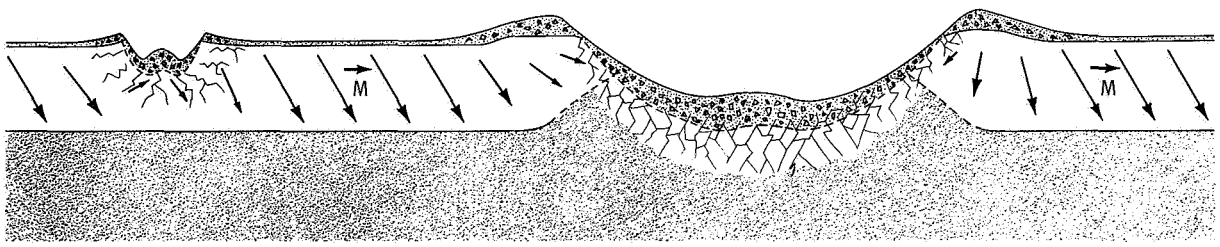

FIGURE 13–8.—Conceptual diagram showing disruption of a previously uniformly magnetized subsurface layer by meteoroid impact. The vectors **M** represent the direction and magnitude of remanent magnetization in the layer.

be postulated for the Apollo 12 and 14 fields. One possibility is that the region was subjected to a uniform magnetic field but that various materials with differing coercivities were magnetized to different strengths. Another model might involve a slow variation in the direction of the ambient field, causing regions that passed through the Curie temperature (ref. 13–21) at different times to be magnetized in different directions.

Models for Magnetizing Lunar Steady-Field Sources

The discovery of magnetic sources on the lunar surface has given strong evidence that, at one time in the lunar past, ambient fields much stronger than at present existed over much or all of the lunar surface. Perhaps the Moon has taken a magnetic snapshot of an early evolutionary phase of the solar system.

Possible origins of the ancient ambient field could have been external to the Moon (Sun or Earth), internal to the Moon (dynamo or thermoelectric currents), or due to induction (eddy currents or unipolar currents). A few possible models are discussed briefly, the first two of which are illustrated in figure 13–9.

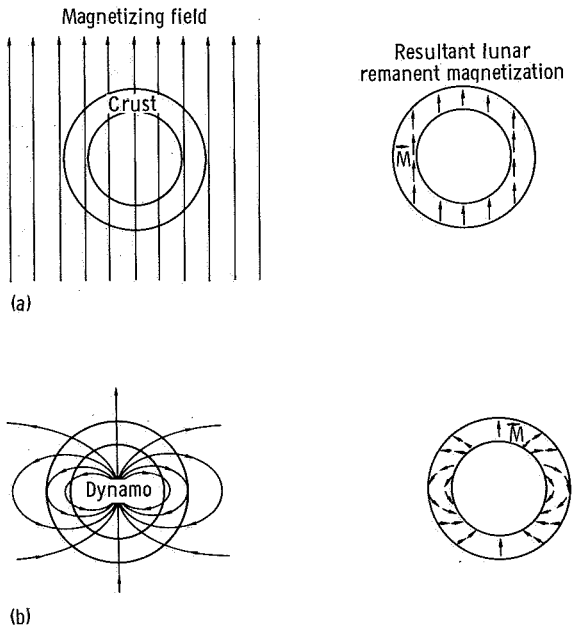

FIGURE 13–9.—Possible magnetic events in lunar history as models for magnetization of near-surface regions of the Moon. The Moon is shown before and after each hypothetical event. The vectors **M** indicate the direction of remanent magnetization in the crustal region. (a) Magnetization by a strong solar or terrestrial field. (b) Lunar internal dynamo field.

Solar field. In this model (fig. 13–9(a)), the Sun generates a magnetic field, stronger than presently exists, which magnetizes the lunar material. The model requires a solar field of constant direction with respect to the solar and lunar spin axes (e.g., solar dipole moment vector pointed out of the solar ecliptic plane) rather than the present-day sector-structure geometry.

Terrestrial field. In this case, the Earth possesses a larger field than in the past (not indicated by paleomagnetic studies), or the Moon has an orbit much closer to the Earth (fig. 13–9(a)). For a terrestrial field of present-day magnitude, the Moon would have had to approach to within 2 to 3 Earth radii R_E (close to the Roche limit (ref. 13–22)) to be subjected to a 10^3-gamma field.

Lunar internal dynamo field. An internal lunar dynamo model (fig. 13–9(b)) requires both a hot core and a sufficient spin rate at the time the surface material cools below the Curie temperature. Past mechanisms for cooling the lunar interior and slowing the spin rate to the present value are also necessary to the dynamo model.

Thermoelectric current field. According to this model, large areas of the Moon were covered at one time by hot lava flows; the temperature gradient between surface and subsurface material induced thermoelectric currents across the interface. The magnetic field associated with this current magnetized the surface material as it cooled below the Curie temperature. It should be kept in mind that these currents would be radial; thus the associated fields would be tangent to the surface and, therefore, would not tend to induce a radial component of magnetization.

Magnetosheath induction of eddy currents. As the Moon passes through the magnetosheath of the Earth during each lunation, it experiences fields that have a preferred direction and are stronger in magnitude than those encountered in the free-streaming solar wind. Repeated passage through the sheath causes an average magnetization to be induced in the direction of flow. For this model, the ancient solar field would have had a geometry

other than the present-day sector structure, because the field reversals across the sector boundary would have tended to average out the magnetizing field over many lunar revolutions.

Solar-wind $\mathbf{v} \times \mathbf{B}$ *induced currents.* The solar wind transports magnetic fields past the Moon at velocities $\mathbf{v}$ of approximately 400 km/sec; the corresponding $\mathbf{v} \times \mathbf{B}$ electric field causes currents to flow along paths of high electric conductivity (refs. 13–23 to 13–25) such as molten mare regions. The fields associated with these currents magnetize these materials as they cool below the Curie temperature. Because this induction mechanism has the strongest influence while the hot region is sunlit, an average preferred direction is associated with $\mathbf{v}$. The $\mathbf{v} \times \mathbf{B}$ induction model also requires some solar-field geometry other than the present-day sector structure.

Preferential selection of any one of the possible models is difficult because available magnetic data represent only a small fraction of the lunar surface. Mapping global geometry and strength of the steady field by future surface and orbital missions should elucidate the "magnetic epoch" of lunar history.

Summary and Conclusions

The Apollo 14 LPM measurements have allowed calculation of vector magnetic fields at two Fra Mauro sites:

(1) Site A: 103 ± 5 gammas, directed 64° down from the horizontal and azimuthally 39° clockwise from due east (fig. 13–7(b))

(2) Site C′: 43 ± 6 gammas, directed 22° down from the horizontal and azimuthally 152° clockwise from due east (fig. 13–7(b))

These sites are separated by a distance of 1.12 km, indicating a 54-gamma/km linear surface-field gradient along a line between the two sites. The data show that local magnetization is not confined to the Apollo 12 site but extends over at least a 180-km region of the Moon and possibly over most of the lunar surface.

The steady fields could be due to a variety of types of sources (e.g., a distant dipole or an extended near-surface platelike region that was originally uniformly magnetized but has subsequently been altered by some mechanism such as meteoroid shock impact). The similarities of magnitudes and directions of the two Apollo 14 measurements and the one Apollo 12 steady-field measurement give preference to the latter model.

References

13–1. DYAL, PALMER; PARKIN, CURTIS, W.; AND SONETT, CHARLES P.: Apollo 12 Magnetometer: Measurement of a Steady Magnetic Field on the Surface of the Moon. Science, vol. 169, no. 3947, Aug. 21, 1970, pp. 762–764.

13–2. STRANGWAY, D. W.; LARSON, E. E.; AND PEARCE, G. W.: Magnetic Studies of Lunar Samples—Breccia and Fines. Proc. Apollo 11 Lunar Sci. Conf., Geochim. Cosmochim. Acta Suppl. 1, vol. 3, 1970, Pergamon Press, Inc., pp. 2435–2451.

13–3. RUNCORN, S. K.; COLLINSON, D. W.; O'REILLY, W.; BATTEY, M. H.; ET AL.: Magnetic Properties of Apollo 11 Lunar Samples. Proc. Apollo 11 Lunar Sci. Conf., Geochim. Cosmochim. Acta Suppl. 1, vol. 3, 1970, Pergamon Press, Inc., pp. 2369–2387.

13–4. DOELL, RICHARD R.; GROMME, C. SHERMAN; THORPE, A. N.; AND SENFTLE, F. E.: Magnetic Studies of Apollo 11 Lunar Samples. Proc. Apollo 11 Lunar Sci. Conf., Geochim. Cosmochim. Acta Suppl. 1, vol. 3, 1970, Pergamon Press, Inc., pp. 2097–2102.

13–5. HELSLEY, C. E.: Magnetic Properties of Lunar 10022, 10069, 10084, and 10085 Samples. Proc. Apollo 11 Lunar Sci. Conf., Geochim. Cosmochim. Acta Suppl. 1, vol. 3, 1970, Pergamon Press, Inc., pp. 2213–2219.

13–6. MIHALOV, J. D.; SONETT, C. P.; BINSACK, J. H.; AND MOUTSOULAS, M. D.: Possible Fossil Lunar Magnetism Inferred From Satellite Data. Science, vol. 171, no. 3974, Mar. 5, 1971, pp. 892–895.

13–7. KEMP, J. C.; SWEDLUND, J. B.; LANDSTREET, J. D.; AND ANGEL, J. R. P.: Discovery of Polarized Light From a White Dwarf. Astrophys. J., vol. 161, no. 2, pt. II, Letters, Aug. 1970, p. 77.

13–8. BRANDT, JOHN C.; AND HODGE, PAUL W.: Solar System Astrophysics. McGraw-Hill Book Co., Inc., 1964.

13–9. NESS, N. F.: Interplanetary Medium. Space Physics, W. N. Hess and G. D. Mead, eds., Gordon & Breach Sci. Pub., 1968, p. 363.

13–10. DYAL, P.; PARKIN, C. W.; SONETT, C. P.; AND COLBURN, D. S.: Electrical Conductivity and Temperature of the Lunar Interior From Magnetic Transient Response Measurements. NASA TM X–62012, 1970.

13–11. SONETT, C. P.; SMITH, B. F.; COLBURN, D. S.; SCHUBERT, G.; AND SCHWARTZ, K.: The

Lunar Electrical Conductivity Profile: Mantle-Core Stratification, Near Surface Thermal Gradient, Heat Flux and Composition. Nature, vol. 230, no. 5293, 1971.

13–12. DOLGINOV, SH. SH.; EROSHENKO, E. G.; ZHUZGOV, L. N.; AND PUSHKOV, N. V.: Investigation of the Magnetic Field of the Moon. Geomagn. Aeron., vol. 1, no. 1, 1961, pp. 18–25.

13–13. DOLGINOV, SH. SH.; PUSHKOV, N. V.; EROSHENKO, E. G.; AND ZHUZGOV, L. N.: Measurements of the Magnetic Field in the Vicinity of the Moon by the Artificial Satellite Luna 10. Dokl. Akad. Nauk SSSR, vol. 170, no. 3, Oct. 31, 1966, pp. 574–577.

13–14. SONETT, C. P.; COLBURN, D. S.; AND CURRIE, R. G.: The Intrinsic Magnetic Field of the Moon. J. Geophys. Res., vol. 72, no. 21, Nov. 1967, pp. 5503–5507.

13–15. NESS, N. F.; BEHANNON, K. W.; SCEARCE, C. S.; AND CANTARANO, S. C.: Early Results From the Magnetic Field Experiment on Lunar Explorer 35. J. Geophys. Res., vol. 72, no. 23, Dec. 1967, pp. 5769–5778.

13–16. BEHANNON, KENNETH W.: Intrinsic Magnetic Properties of the Lunar Body. J. Geophys. Res., vol. 73, no. 23, Dec. 1968, pp. 7257–7268.

13–17. GEYGER, W. A.: Nonlinear-Magnetic Control Devices. McGraw-Hill Book Co., Inc., 1964.

13–18. GORDON, D. I.; LUNDSTEN, R. H.; AND CHIARODO, R. A.: Factors Affecting the Sensitivity of Gamma-level Ring-core Magnetometers. IEEE Trans. Magn., vol. MAG–1, no. 4, Dec. 1965, pp. 330–337.

13–19. BARNES, A.; CASSEN, P.; MIHALOV, J. D.; AND EVIATOR, A.: Permanent Lunar Surface Magnetism and Its Deflection of the Solar Wind. Science, vol. 171, 1971.

13–20. DYAL, P.; PARKIN, C. W.; AND SONETT, C. P.: Lunar Surface Magnetometer Experiment. Sec. 4 of Apollo 12 Preliminary Science Report. NASA SP–235, 1970.

13–21. NAGATA, TAKESI: Rock Magnetism. Maruzen Co., Ltd. (Tokyo) (Plenum Press (New York) exclusive U.S. distributor), 1961.

13–22. INGLIS, F. J.: Planets, Stars, and Galaxies. John Wiley & Sons, Inc., 1968.

13–23. SONETT, C. P.: Principle of Planetary Unipolar Generators. Vol. II of Planetary Electrodynamics, ch. VII–11, Samuel C. Coroniti and James Hughes, eds., Gordon & Breach Sci. Pub., 1969, pp. 373–378.

13–24. SCHUBERT, G.; AND SCHWARTZ, K.: A Theory for the Interpretation of Lunar Surface Magnetometer Data. The Moon, vol. 1, 1969.

13–25. SILL, W. R.; AND BLANK, J. L.: Method for Estimating the Electrical Conductivity of the Lunar Interior. J. Geophys. Res., vol. 75, no. 1, Jan. 1970, pp. 201–210.

ACKNOWLEDGMENTS

The authors wish to express deep appreciation for the effort expended by all the personnel connected with this experiment. In particular, thanks are extended to the subcommittee and steering committee chairmen who modified and added this new experiment to their agenda for consideration. The authors wish to acknowledge, in particular, Carle Privette, Michael Dix, Donald Mulholland, Glen Goodwin, Ernest Iufer, Robert Murphy, and Kathy Stark of the NASA Ames Research Center; and J. B. Thomas of the NASA Manned Spacecraft Center. The diligent efforts of these and many others brought success to this experiment. Special thanks are extended to Dr. David S. Colburn of the NASA Ames Research Center for use of Explorer 35 data.